

Simulation of γ' Precipitation Kinetics in a Commercial Ni-Base Superalloy

M.G. FAHRMANN^{1,2} and D.A. METZLER¹

1.—Haynes International Inc., 1020 West Park Avenue, Kokomo, IN 46904, USA. 2.—e-mail: mfahrmann@haynesintl.com

The ability to accurately simulate the precipitation kinetics of γ' and other strengthening phases in Ni-base superalloys is of great interest to industry. Several commercial simulation tools such as TC-PRISMA (Thermo-Calc, Sweden) and PanPrecipitation (CompuTherm, USA) have been made available in recent years. This paper reports the outcome of a validation study on wrought Ni-base superalloy HAYNES[®] 282[®] alloy for two scenarios of commercial interest: (1) the precipitation of γ' during continuous cooling, and (2) the precipitation of γ' during two-step aging. The simulation results are validated against experimental data. Any discrepancies are discussed in the context of the uncertainty in key material properties (such as interfacial energies), model assumptions, and experimental errors.

INTRODUCTION

The calculation of phase equilibria in multi-component commercial superalloys by means of CALPHAD software (Thermo-Calc, Pandat, ChemSage, etc.) is commonplace in the superalloys industry. However, simulations of the important precipitation kinetics of major strengthening phases in these alloys, most notably γ' , are comparatively still at their infancy in industry. This is partly because, until recently, commercial simulation tools have not been available.^{1,2} Also, confidence in the fidelity of these new simulation tools needs to be built over time. This requires extensive validation, most importantly on commercial alloys.

This study compares measured average γ' sizes with simulated ones for two relevant heat-treating scenarios of new wrought γ' -strengthened HAYNES 282 alloy: (1) continuous cooling from annealing temperatures, and (2) the alloy's recommended 2-step aging cycle. This particular alloy was chosen because its chemical composition and phase constitution fall well into validated CALPHAD space. Moreover, the composition of the alloy in wrought form is reasonably uniform. Lastly, the homogeneous precipitation of intragranular γ' , which is consistent with model assumptions and the basis of the alloy's strength, was the focus of this study.

EXPERIMENTAL DETAILS

The studied material originated from a production heat of 282 alloy. The alloy's nominal composition is given in Table I. The product form was a hot-rolled bar in the mill-annealed condition (1135°C). For the cooling rate study, samples were re-heated in an argon-shielded tube furnace to 1150°C for 5 min, and then cooled in a controlled fashion to less than 500°C at cooling rates ranging from 1 to 950°C/min.³ For the two-step aging study, samples were aged in a laboratory muffle furnace at 1010°C for 2 h, rapidly air-cooled, and then aged for an additional 8 h at 788°C, followed by another rapid air cool.

The samples were sectioned and prepared using standard metallographic techniques. The γ' phase was revealed by electrolytic etching with Radavich's etch.⁴ The γ' precipitates were imaged in FEG-SEMs utilizing the high-resolution in-lens signal. The precipitate size was equated to the radius of an area-equivalent circle in the 2D images. Several precipitates (~100–600) were measured to calculate the average precipitate radius. Digitized images (each containing an embedded scale reference marker) were thresholded using ImageJava software.⁵ Mean precipitate sizes and distributions were characterized using the Analyze Particles tool in ImageJava. When multi-modal size distributions were apparent on the micrographs, only the coarsest

population was evaluated. Since the samples were deep-etched, stereological correction for particle slicing effects was not deemed necessary. Ninety-five percent confidence limits for mean precipitate size were approximately $\pm 3\%$ of the mean.

The starting point for the simulations was the assumption of the annealed samples being in thermodynamic equilibrium. This assumption is important since the composition of the matrix phase, from which γ' precipitates form during cooling and aging, will differ from the material's bulk composition. In particular, titanium and carbon contents will be lower due to a significant portion of these elements being tied up in primary MC carbides. The matrix composition was calculated using Thermo-Calc in conjunction with ThermoTech's Ni-DATA database v.8.

The precipitation simulations were executed on a core i5 64-bit PC using both Thermo-Calc's TC-PRISMA v.2.0 precipitation module^{6,7} and the PanPrecipitation2014 module of the PANDATTM software.^{8,9} Simulation time was typically less than 1 h. Key model assumptions, as verified by experiment, were:

- the homogeneous nucleation of γ' in the bulk of the grains,
- an isotropic γ/γ' interfacial energy,
- a negligible strain energy contribution to the nucleation barrier of γ' .

The material parameters used in the simulations were $7.1 \times 10^{-6} \text{ m}^3$ for the molar volumes of both, the γ matrix and the γ' precipitates, based on a corresponding lattice parameter of $3.6 \times 10^{-10} \text{ m}$,¹⁰ a nucleation site parameter of 0.001, and a driving force factor of 1.0. The crucial interfacial energy was varied parametrically between 10 and 80 mJ/m^2 , a range that encompasses interfacial energy values derived from coarsening studies in model $\gamma-\gamma'$ alloys.^{11,12}

RESULTS AND DISCUSSION

Precipitation of γ' During Continuous Cooling

The evolution of the γ' precipitate number density upon continuous cooling at a rate of 1°C/min is shown in Fig. 1, assuming a γ/γ' interfacial energy of 20 mJ/m^2 . Notice that γ' did not form in this

Table I. Nominal chemical composition (in wt.%) of HAYNES 282 alloy

<u>Ni</u>	<u>Co</u>	<u>Fe</u>	<u>Cr</u>	<u>Mo</u>	<u>Mn</u>	<u>Al</u>	<u>Ti</u>	<u>C</u>	<u>B</u>
Bal.	10	1.5 ^a	20	8.5	0.3 ^a	1.5	2.1	0.06	0.005

^aMaximum.

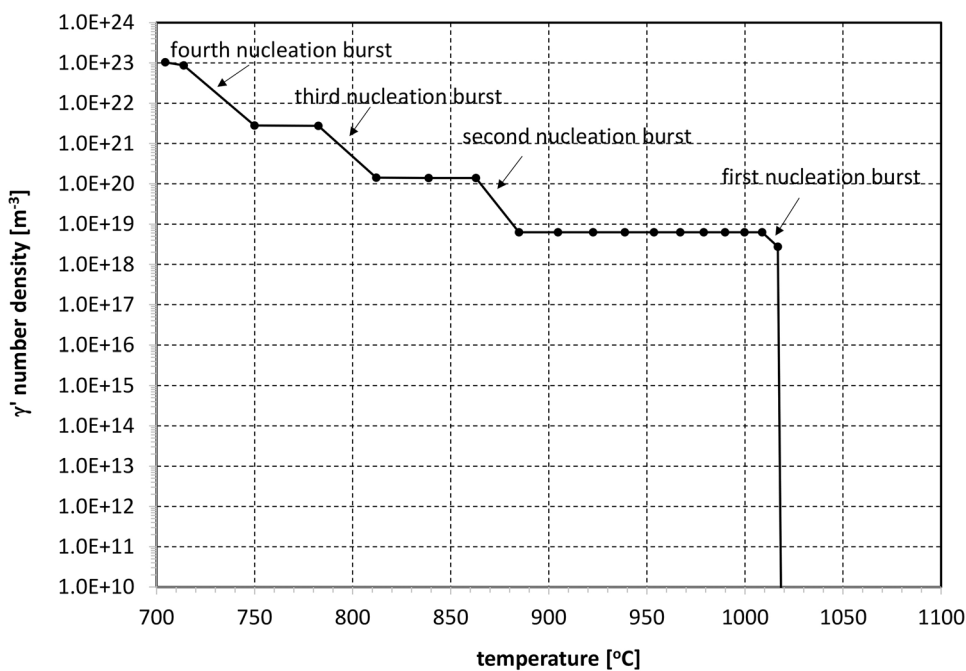


Fig. 1. PanPrecipitation2014 simulation of the evolution of the number density of γ' in the course of continuous cooling of HAYNES 282 alloy. The cooling rate was 1°C/min from 1093°C to 704°C . Gamma/gamma-prime interfacial energy is assumed to be 20 mJ/m^2 . Kampmann-Wagner-Numerical (KWN) model.¹⁴

PANDAT simulation (subsequently referred to as PanPrecipitation 2014 simulations) until the temperature dropped below 1020°C. This temperature is close to the γ' solvus temperature of 1000°C in the 282 alloy. Due to the slow cooling rate, there is virtually no undercooling effect. Notice also several nucleation bursts as indicated by the jumps in nucleation density on this logarithmic scale. At least a bi-modal γ' size distribution was indeed observed for this cooling rate, as evident from Fig. 2.

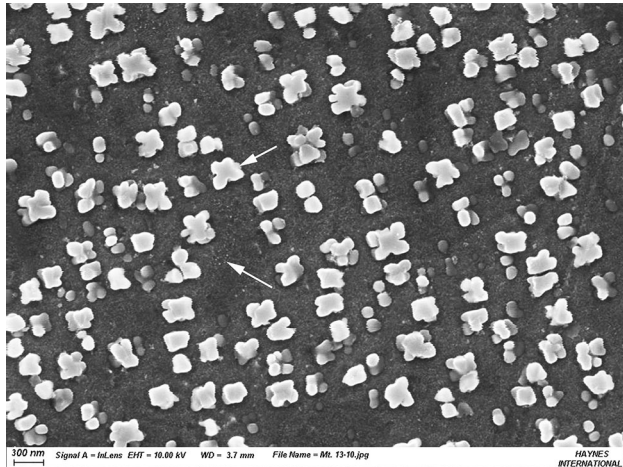


Fig. 2. SEM in-lens micrograph of the dispersion of γ' precipitates resulting from continuous cooling of HAYNES 282 alloy at 1°C/min. Two distinctly different size classes (white arrows) are discernible.

These simulated nucleation events resulted in the evolution of the average γ' radius in Fig. 3. Just before the second nucleation burst at 885°C, the precipitates formed during the first burst are simulated to have grown to a size of 185 nm. It is this average size of the coarsest population that was measured. Subsequent nucleation bursts caused a decrease in the simulated average γ' size due to much smaller precipitates being formed at these lower temperatures.

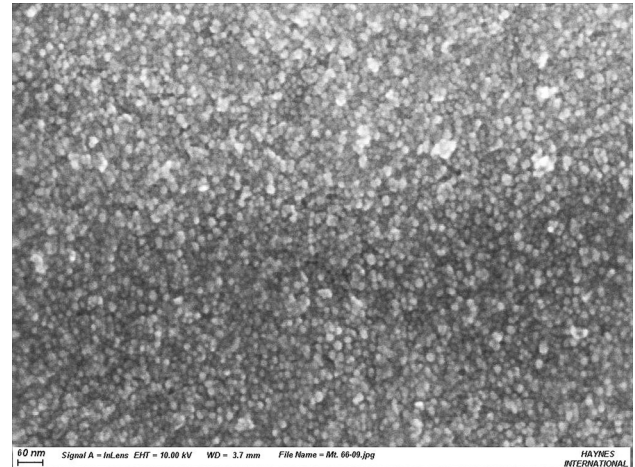


Fig. 4. SEM in-lens micrograph of the dispersion of γ' precipitates resulting from continuous cooling of HAYNES 282 alloy at 300°C/min.

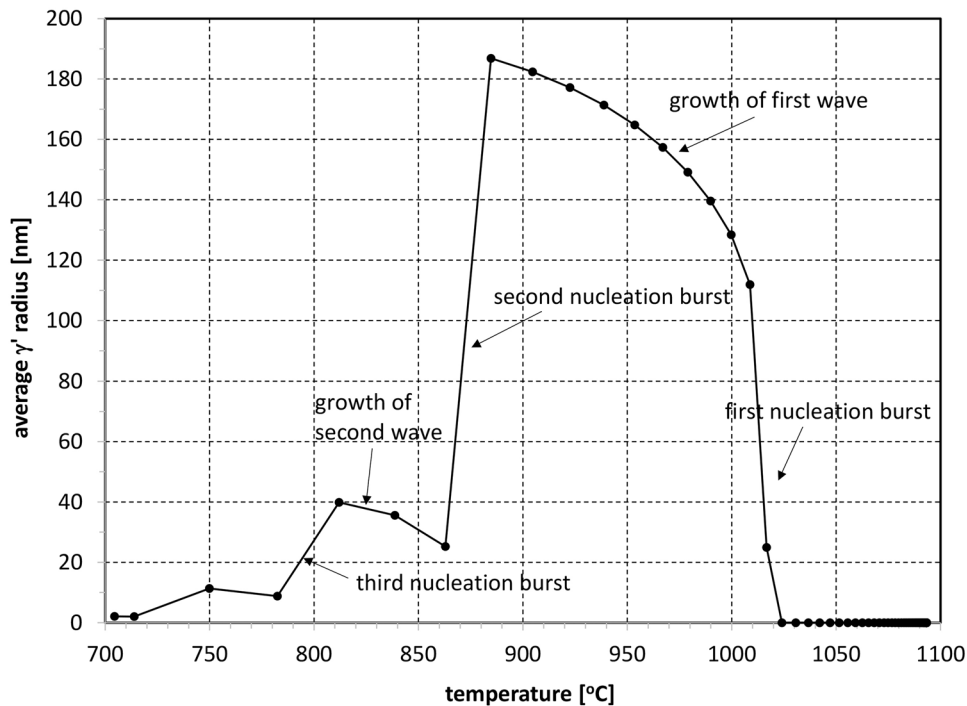


Fig. 3. PanPrecipitation2014 simulation of the evolution of the average γ' radius in the course of continuous cooling of HAYNES 282 alloy. The cooling rate was 1°C/min from 1093°C to 704°C. γ/γ' interfacial energy is assumed to be 20 mJ/m². KWN model.

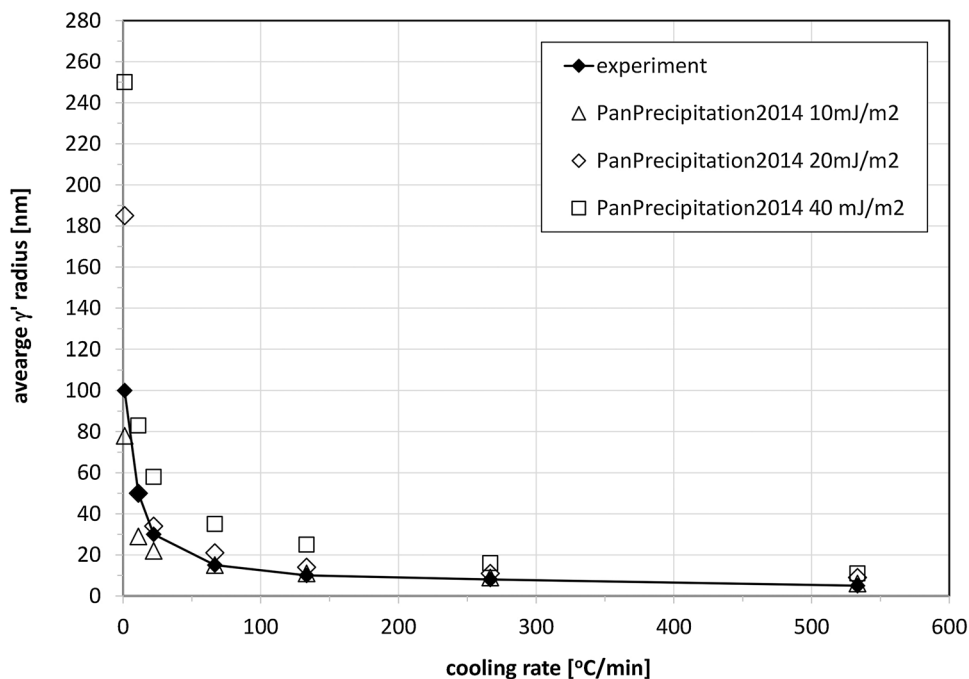


Fig. 5. Comparison between the experimentally determined average γ' radius and simulated average radii as a function of cooling rate in HAYNES 282 alloy for different values of the γ/γ' interfacial energy. Only the coarsest predicted gamma-prime population is compared to experiment. Experimental uncertainty is on the order of the size of the symbols.

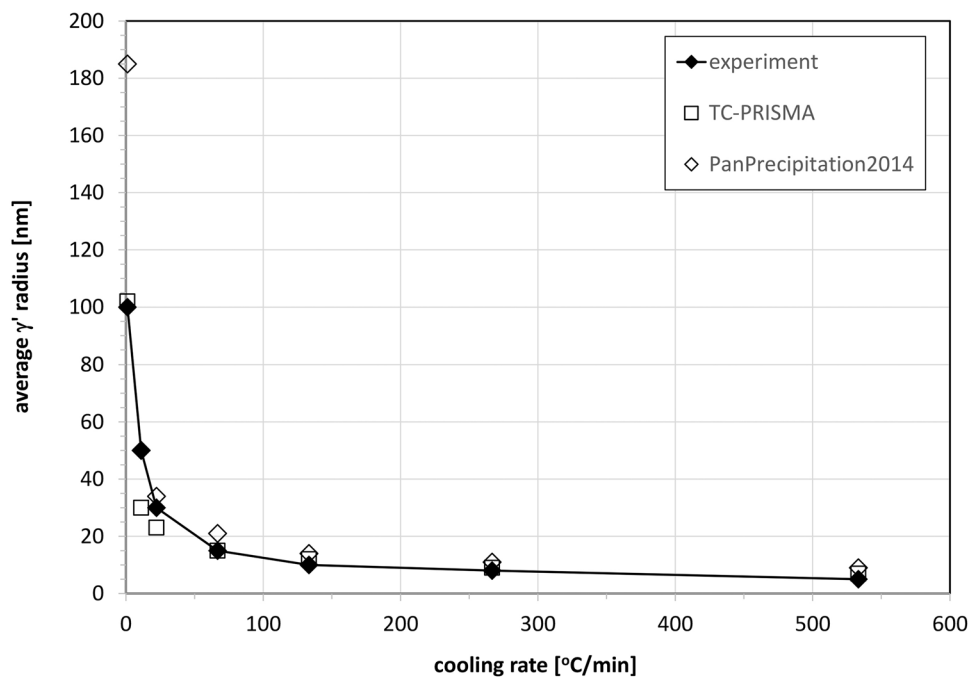


Fig. 6. Comparison between the experimentally determined average γ' radius and simulated average radii (PanPrecipitation2014 and TC-PRISMA) as a function of cooling rate in HAYNES 282 alloy for a γ/γ' interfacial energy of 20 mJ/m². Only the coarsest predicted γ' population is compared to experiment. Experimental uncertainty is on the order of the size of the symbols.

At much higher cooling rates, for example 200 $^{\circ}\text{C}/\text{min}$, multi-modal γ' size distributions are still being predicted. However, the sizes of the finer populations are well below 10 nm, which is considered to

be the resolution limit of the in-lens detector in the SEMs used. As expected, precipitates are small (Fig. 4). Their spherical shape strongly suggests that the γ/γ' interfacial energy was isotropic.

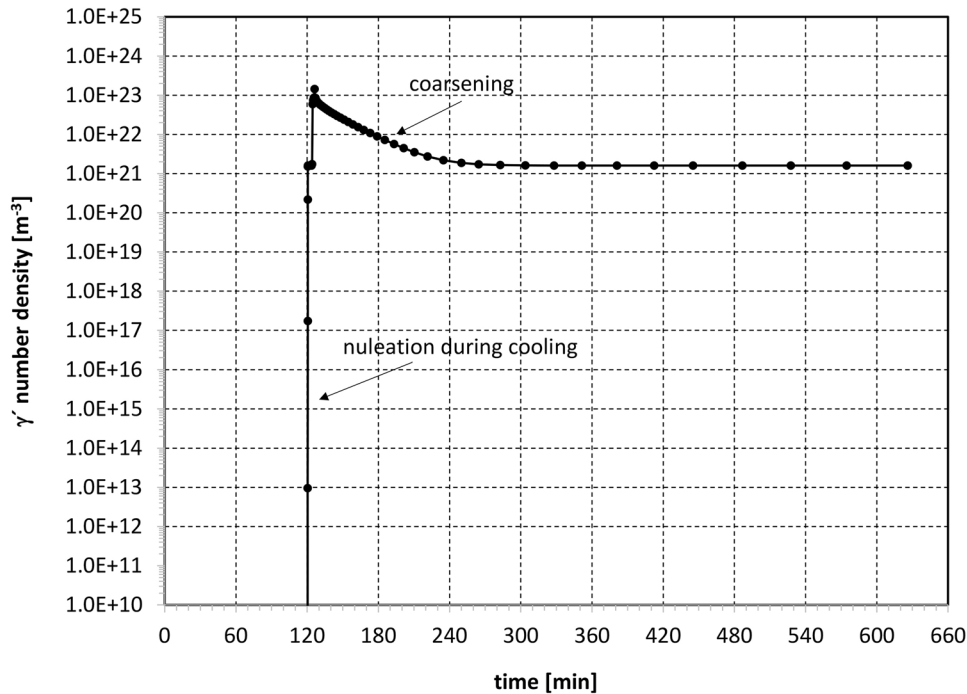


Fig. 7. PanPrecipitation2014 simulation of the evolution of γ' number density in the course of two-step aging of HAYNES 282 alloy, assuming a 6-min cooling leg between the first aging temperature of 1010°C and the second aging temperature of 788°C. γ/γ' interfacial energy is assumed to be 20 mJ/m². KWN model.

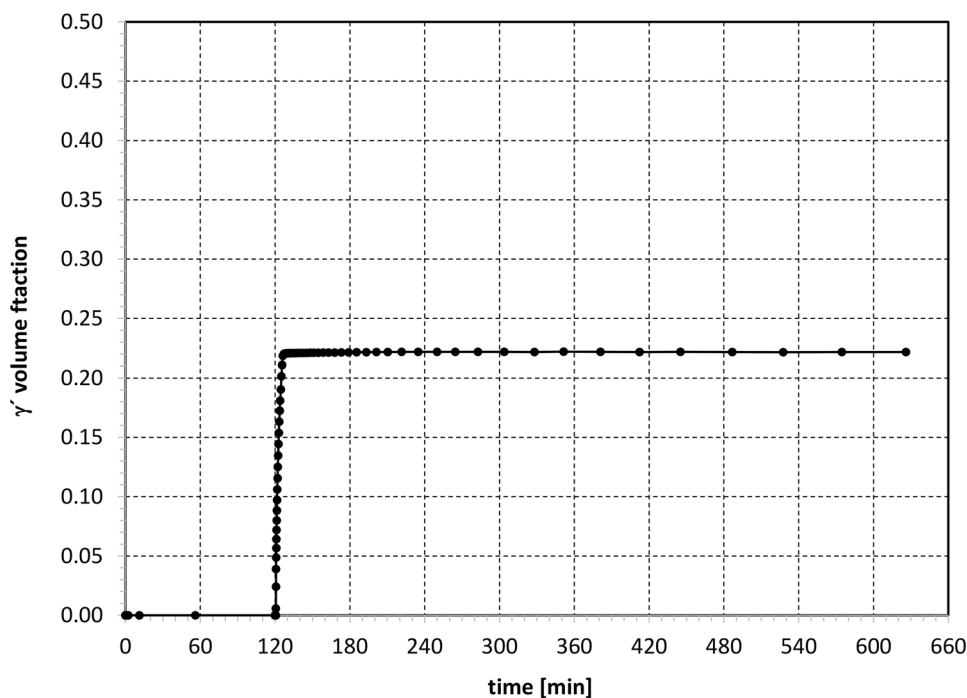


Fig. 8. PanPrecipitation2014 simulation of the evolution of γ' volume fraction in the course of two-step aging of HAYNES 282 alloy, assuming a 6-min cooling leg between the first aging temperature of 1010°C and the second aging temperature of 788°C. γ/γ' interfacial energy is assumed to be 20 mJ/m². KWN model.

The PanPrecipitation2014 simulation results are compared to the measured values in Fig. 5, with interfacial energy being the curve parameter. The

simulations correctly reflect the steep initial drop in average γ' size. One complicating factor at the slowest cooling rate is the non-spherical shape of

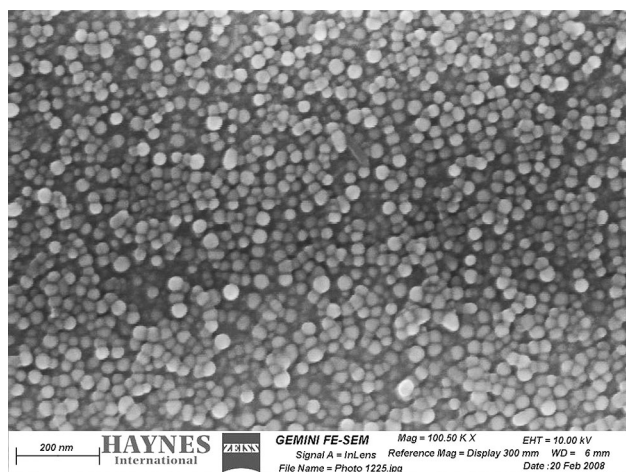


Fig. 9. SEM in-lens micrograph of the dispersion of γ' precipitates resulting from two-step aging of HAYNES 282 alloy. Deep etch.

the precipitates, potentially invalidating the model assumptions. Precipitate shape tended to be spherical at all other cooling rates studied, indicative of a very small γ/γ' lattice mismatch. Disregarding the slowest cooling rate data point, it appears that a value of 20 mJ/m^2 resulted in the best match with experiment. This value agrees quite well with that of $(22 \pm 7) \text{ mJ/m}^2$ derived from γ' coarsening studies in a γ - γ' Ni-Al-Cr model alloy by Sudbrack et al.¹²

Finally, in Fig. 6, we compare the simulation results of PanPrecipitation2014 and TC-PRISMA for the same interfacial energy of 20 mJ/m^2 . Except for the slowest cooling rate, differences are minor, particularly in view of the experimental uncertainty. This is not too surprising since both software packages are based on the same underlying models,^{13,14} and both draw on the same mobility data developed by NIST.¹⁵ Remaining differences could be due to the different thermodynamic databases used, as manifested by different γ' solvus temperatures predicted for this alloy (1020°C with PANDAT versus 1005°C with Thermo-Calc). The outcome of these simulations is quite relevant to industry. For example, it would allow the simulation of the formation of cooling γ' in larger section-size components based on the local cooling history.

Precipitation of γ' During Two-Step Aging

The outcome of a PanPrecipitation simulation of the alloy's particular two-step aging cycle, using again a value of 20 mJ/m^2 for the interfacial energy and assuming a 6-min cool-down from the higher to the lower of the aging temperatures, is shown in Fig. 7. This 6-min cool-down (corresponding to $37^\circ\text{C}/\text{min}$) would reflect the cooling history of the center of larger section-size products during a rapid air cool.¹⁶ Notice also that the alloy is typically cooled to room temperature before being heated back up to the second aging temperature. Thus, any additional

nucleation events below the lower aging temperature were neglected. According to the simulations, nucleation would already be complete by the time the material has been cooled to the lower aging temperature. In fact, it appears that precipitate coarsening commences at the beginning of the second aging step. Hence, the equilibrium volume fraction γ' would virtually be established at the beginning of the second aging step (Fig. 8).

For the same cooling scenario, the predicted average γ' radii after 8 h of aging at the lower temperature are 20 nm (TC-PRISMA) and 30 nm (PanPrecipitation2014), respectively. Again, we suspect that this difference is largely due to differences in the respective thermodynamic databases and the resultant differences in the driving force of γ' precipitation. The predicted average aging γ' size is also sensitive to the cooling rate through the γ' precipitation range from the higher to the lower aging temperature; for example, the predicted average aging γ' radius is only 15 nm for a 0.6-min duration cooling leg. This duration is more compatible with cooling of small samples in the laboratory, and the value agrees very well with the measured value of 15 nm. We also note that both simulation tools predicted mono-modal γ' size distributions consistent with experimental observations (Fig. 9).

As with the cooling rate scenarios, such simulation capability is of great commercial interest because it allows simulation of the local evolution of γ' in larger section-size, complex-shaped parts upon heat treating. These local average γ' sizes could be fed into property prediction models such as JMatPro in order to assess local part properties and conformance to applicable part specifications. We emphasize that a significant initial investment beyond the purchase of the simulation software needs to be made before being able to fully capitalize on it, which encompasses dialing-in of alloy-dependent critical material parameters by calibration against accurate experimental data.

CONCLUSION

1. The commercial precipitation simulation tools TC-PRISMA and PanPrecipitation2014 were utilized to simulate two heat treating scenarios of wrought HAYNES 282 alloy: (1) continuous cooling from annealing temperatures, and (2) two-step aging.
2. Given certain assumptions, the simulations correctly predicted the trends in resultant average γ' sizes and modalities in size distributions. For this alloy, the best match with experiment was obtained for a γ/γ' interfacial energy of 20 mJ/m^2 .
3. This validation study indicates the capabilities of this relatively new suite of tools, and their potential to aid in the solution of industrially relevant problems.

REFERENCES

1. G.B. Olson, H.-J. Jou, J. Jung, J.T. Sebastian, A. Misra, I. Locci, and D. Hull, *Proceedings of the Eleventh International Symposium on Superalloys*, ed. R.C. Reed, (Warrendale, PA: TMS, 2008), p. 923.
2. K. Wu, F. Zhang, S. Chen, W. Cao, and Y.A. Chang, *Proceedings of the Eleventh International Symposium on Superalloys*, ed. R.C. Reed, (Warrendale, PA: TMS, 2008), p. 933.
3. B. Alexandrov, J. Rodelas, M. Kittila, J. Lippold, and D.A. Metzler, Oral Presentation, MS&T 2011 (Columbus, OH, 2011).
4. J.F. Radavich, *Proceedings of the Symposium on Superalloys 718, 625, 706 and Various Derivatives*, ed. E.A. Loria, (Warrendale, PA: TMS, 1997), p. 17.
5. W.S. Rasband, ImageJ, U.S. National Institutes of Health, Bethesda, MD, <http://imagej.nih.gov/ij/>, 1997–2016. Accessed 12 Mar 2011.
6. Q. Chen, H.J. Jou, and G. Sterner, TC-PRISMA User's Guide and Examples. Thermo-Calc Software AB, Stockholm, Sweden. <http://www.thermocalc/media/40970/Precipitation-Module-TC-PRISMA-User-Guide.pdf>. Accessed 10 May 2014.
7. Q. Chen, K. Wu, G. Sterner, and P. Mason, *J. Mater. Eng. Perform.* 23, 4193 (2014). doi:10.1007/s11665-014-1255-6.
8. S.L. Chen, S. Daniel, F. Zhang, Y.A. Chang, X.Y. Yan, F.Y. Xie, R. Schmid-Fetzer, and W.A. Oates, *CALPHAD* 26, 175 (2002).
9. W. Cao, S.L. Chen, F. Zhang, K. Wu, Y. Yang, Y.A. Chang, R. Schmid-Fetzer, and W.A. Oates, *CALPHAD* 33, 328 (2009).
10. J.P. Cotner, Haynes International Inc., Kokomo, IN, unpublished research, 2010.
11. A.J. Ardell, *Met. Trans. A* 1, 525 (1970).
12. C.K. Sudbrack, R.D. Noebe, and D.N. Seidman, *Acta Mater.* 55, 119 (2007).
13. J.S. Langer and A.J. Schwartz, *Phys. Rev. A* 21, 948 (1980).
14. R. Wagner and R. Kampmann, in *Decomposition of Alloys: The Early Stages*, ed. P. Haasen, V. Gerold, R. Wagner and M.F. Ashby, (Oxford, Great Britain: Pergamon, 1984), p. 91.
15. C.E. Campbell, W.J. Boettinger, and U.R. Kattner, *Acta Mater.* 50, 775 (2002).
16. D.A. Metzler, Haynes International Inc., Kokomo, IN, unpublished research, 2015.